JOINT INSTITUTE FOR NUCLEAR RESEARCH
Frank Laboratory Of Neutron Physics

FINAL REPORT ON THE START PROGRAMME

On The Reflection of Neutrons and X-ray from Multilayered Structures

Supervisor
Dr. Vladimir Zhaketov

Student
Omar Ahmed Hassan

University Of Science and Technology at Zewail City,
6th Of October, Egypt

Participation Period
September - November
Summer Session 2022

Dubna, 2022

Abstract

This document is a two-part report summarizing the knowledge acquired and applied during a two month research experience in the Laboratory of Neutron Physics at the Joint Institute for Nuclear Research. The first part is a background theoretical foundation for all the experimental and computational work that was carried out. The second part is an illustration of the real-time experience and methodology including plans, progress, results, questions that arose and answers that were proposed and some that were applied.

Contents

1 Neutron Waves

1.1 Introduction

The theoretical part of this report is heavily based on the "Handbook of Neutron Optics" [1]. It is to be considered for the most part a concise review of parts of chapters of the book that are of relevance to the methodology. The knowledge is constructed starting from the fundamental wave behaviour of matter and up to the calculational frameworks, modelling techniques and experimental methods. As the topics of the conducted research are mainly on the reflection and transmission of neutrons (and X-ray) through multilayered structures the parts of discussions concerning diffraction and interference are kept at a minimum. It is difficult to do right by this sub-field of physics in giving it descriptive words that show its marvellous nature. From being a probe to questions and heuristics of fundamental physics that leads only to enlightenment and discovery to being a method of a wide range of applications between the science of materials and biophysical research. It's only appropriate to quote from the words of the writer of the book.

"Genuine is relativity theory,
Great is field theory and the physics of elementary particles,
Stars capture imagination,
But nothing in the world is as interesting as neutron optics." V. Ignatovich.

1.2 Wave Behaviour of Particles

The amalgamation of particle motion and wave propagation was first discovered by *de Broglie* in 1925. His argument for the basic construction of a relation between the two fundamental properties describing both forms of motion namely *momentum* for the motion of a point mass and *wavelength* for the travelling of disturbances were based on the combination of two fundamental ideas that were discovered in the beginning of the 19th century. The first idea was the equivalence of mass and energy as a consequence of the theory of relativity discovered by Einstein and the second is the idea of radiation quanta discovered by Planck. If we describe a particle in its rest frame by a function in the form of a wave $sin[2\pi\nu_0(t_0-\tau_0)]$ where t_0 is the proper time for the particle, ν_0 is the rest frame frequency of oscillation, τ_0 is a constant and the wave has the same phase at each point in space since the particle is at rest (if it had an oscillation in space at a given time this oscillation will move at the next instant from one point to the next and such behavior is that of a moving wave which is counter to the proposal that we are considering the rest frame of the particle), to observe the behaviour of the wave as it is moving one can consider a frame moving relative to the particle. According the Lorentz transformation for the time component of the space-time four vector

$$t_0 = \frac{t-\frac{\beta x}{c}}{\sqrt{1-\beta^2}} \tag{1}$$

Therefore in this frame the wave is oscillating both in time and in space (travelling wave) in accordance with the following function

$$sin[2\pi\frac{\nu_0}{\sqrt{1-\beta^2}}(t-\frac{\beta x}{c}-\tau_0)] \tag{2}$$

with frequency $\nu=\frac{\nu_0}{\sqrt{1-\beta^2}}$. The phase velocity V can be read from the argument of the sinusoidal function $V=\frac{c}{\beta}=\frac{c^2}{v}$. One can also define a group velocity for a superposition of such waves all with frequencies in the proximity of

v. In this case the wave velocity of the resultant amplitude is given by the Rayleigh definition $U = \frac{\partial \omega}{\partial k}$.

$$\frac{1}{U} = \frac{\partial v \frac{\beta}{c}}{v} = \frac{1}{c\beta} = \frac{1}{v} \tag{3}$$

Therefore the group velocity is the same as that of the particle velocity. Using Planck's energy relation for radiation quanta $E = hv$ and the equivalence of mass and energy $E = m_0 c^2$ the relation between the mass and frequency for the particle at its rest frame is $m_0 = \frac{hv_0}{c^2}$. Since the momentum of the particle p is given by $p = \frac{m_0 v}{\sqrt{1-\beta^2}}$ we have a relationship between the momentum of the particle and its frequency (and wavelength) through the rest mass

$$p = \frac{(\frac{hv_0}{c^2})v}{\sqrt{1-\beta^2}} = \frac{hvv}{c^2} = \frac{hv}{V} = \frac{h}{\lambda} \tag{4}$$

1.3 Observation of Neutron's Wave Nature

Following the discovery of neutrons in 1932 experiments were carried out to verify its wave nature. As neutrons are electrically neutral and of much larger mass compared to electrons (where the first wave nature of particles were observed) they have a significant advantage in terms of energy requirements in experiments (slower neutrons can have the same wavelength as that of much faster electrons) and the ability to traverse through solid crystals with negligible electrical interaction between electron clouds where the only source of interaction potential between an incident beam of neutrons and the crystal is through atomic nuclei which results in the appearance of sharp and obvious Bragg peaks from scattered neutrons. A basic setup for such experiment is to have a radioactive element (ex. Rn) submerged in a moderator that slows down produced neutrons (usually paraffin or water with deuterium hydrogen), slits of a neutron absorbing material (ex. cadmium) to produce a beam of neutrons as they pass through, a rotatable sample on to which the neutron beam can be incident on variable angles, and a neutron counter/detector (ex. devices that detect ionizing byproducts of the interaction between the incident neutrons and a strong neutron absorbers inside the detector as BF3 gas-filled proportional detector). The count rate of detector is substantially higher when the neutrons are incident at an angle that results in constructive interference of the reflected beam from different atomic planes in the structure.

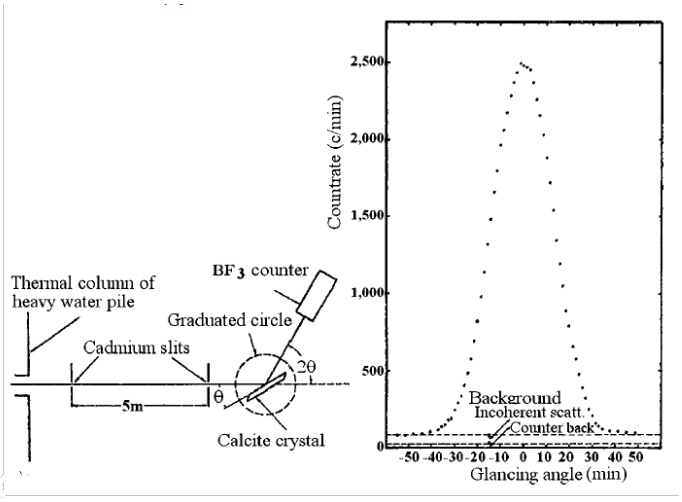

Figure 1: A typical experiment for the observation of neutrons' Bragg scattering

1.4 Time of Flight

An experimental technique worth mentioning as it was used for the determination and selection of wavelengths of neutrons in the conducted experiments is the analysis of the time of flight of neutrons. The time of flight analysis invokes the particle nature of neutrons in order to determine the corresponding wavelength of the neutron wave. If a monochromatic neutron beam were to travel a fixed distance L at a time T we have the following relation $m\frac{L}{T} = \frac{h}{\lambda}$ therefore by measuring the time of the neutrons' flight we can determine the wavelength of the neutron beam by the relation

$$\lambda = \frac{h}{mL}T \tag{5}$$

Obtaining a beam of a given wavelength can be achieved mechanically by using two discs of absorbing materials. Each of the two discs contain a slit opening. The two discs are connected together by a rod at a certain distance apart d. The slit of the second disk is not aligned with the first disk but rather at an offset angle relative to the first slit. Now as the rod rotates neutrons that pass through the first disk's slit will be blocked by the second disk unless they travel at a particular velocity that allows them to arrive at the second disk (traveling a distance d) just as the second slit is passing by so that they can pass through it too. This method is used as a *mechanical velocity selector* resulting in a neutron beam of a narrow spectral range.

2 Wave Mechanics of Neutrons

2.1 Introduction

Having established the wave behaviour of neutrons doors are open to examine all optical phenomena that are characteristic of waves namely reflection, refraction, diffraction and interference however the scope of the analysis of interest is only that of the reflection and refraction of neutrons. A neutron is a superposition of many plane waves (a wave packet) each with a wave function

$$\Psi(\vec{r},t) = e^{i(\vec{k}\cdot\vec{r}-\omega t)} \tag{6}$$

Each plane wave is a momentum eigenstate ($\vec{p} = \hbar\vec{k}$) of the neutron, and $\omega = \frac{E}{\hbar}$. The premise of the analysis is that by analysing the behaviour of a single plane wave (which of itself cannot be a physical particle because it is not normalizable) one can understand the behaviour of a superposition of them namely the wave packet representing the neutron. The schrodinger equation for the wave packet reads

$$i\hbar\frac{\partial\Psi(\vec{r},t)}{\partial t} = \frac{\hbar^2}{2m}[-\nabla^2 + u(\vec{r},t)]\Psi(\vec{r},t) \tag{7}$$

Where $\frac{\hbar^2 u}{2m}$ is the interaction potential between neutrons and matter. We only consider time-independent potentials so by using separation of variables we have $\Psi(\vec{r},t) = e^{i\omega t}\phi(\vec{r})$. Since we also only study planar systems that are symmetric in the y-z plane and change only along the x-direction we can further separate the wave function into plane waves in the y-z plane and a single scalar function of x $\Psi(\vec{r},t) = e^{i\omega t}e^{i\vec{k}_\parallel\cdot\vec{r}_\parallel}\psi(x)$ Where $\parallel$ symbolizes the components of the vectors in the y-z plane. The one dimensional time-independent Schrodinger equation therefore is

$$[\frac{d^2}{dx^2} - u(x) + k_x^2]\psi(x) = 0 \tag{8}$$

Where $k_x = \sqrt{k^2 - k_\parallel^2}$ is the x-component of the wave vector. Since our analysis will be mainly concerned with this component we will simply call it k for the following parts.

2.2 Potential Step

The first step is to analyze the propagation of the neutrons as they encounter a potential step from their original vacuum propagation. In this situation the neutrons encounter an infinitely thick material where a part of the wave is reflected and a part is transmitted through the potential. Such encounter for the neutrons in the context of multilayered structures will model the reflection of the neutron from the *substrate* upon which the structure is sat. If the potential is stepped up from 0 to u_0 at the point $x = 0$ the Schrodinger equation becomes

$$[\frac{d^2}{dx^2} - u_0\Theta(x > 0) + k^2]\psi(x) = 0 \tag{9}$$

Where $\Theta(x)$ is 1 when the logical argument x is true and 0 otherwise

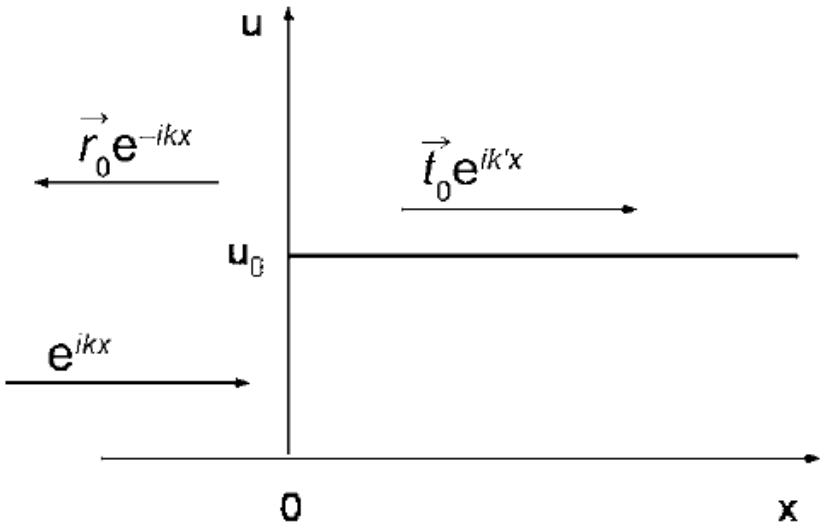

Figure 2: Step Potential

As seen from the previous figure the wave function can be written in terms of two unknown amplitudes as

$$\psi(x) = \Theta(x \leq 0)[e^{ikx} + \vec{r_0}e^{-ikx}] + \theta(x > 0)[\vec{t_0}e^{ik'x}] \tag{10}$$

Where k' is the wave vector inside the material and the arrows on top indicate that the incident wave towards the interface travels from left to right. By substituting the transmitted part in the Schrodinger equation we have a formula for k' which is an expression of the conservation of energy $k'^2 = k^2 - u_0$. To find the amplitudes $\vec{r_0}$ and $\vec{t_0}$ we employ the continue of the Schrodinger equation and its first derivative at x=0 arriving at the two equations

$$1 + \vec{r_0} = \vec{t_0} \tag{11}$$

$$k[1 - \vec{r_0}] = k'\vec{t_0} \tag{12}$$

The solution for the two amplitudes in terms of the wave vectors is

$$\vec{r_0} = \frac{k - k'}{k + k'} \tag{13}$$

$$\overrightarrow{t_0} = \frac{2k}{k+k'} \tag{14}$$

The reflectivity of the neutrons is the square of the reflection amplitude. For $k^2 >> u_0$, k' can be Taylor expanded as $k' = \sqrt{k^2 - u_0} \approx k - \frac{u_0}{2k}$. In such case the reflectivity is given by $|\overrightarrow{r_0}|^2 = \frac{|u_0|^2}{16k^4}$. If $k^2 < k_c^2$ where $k_c = \sqrt{u_0}$ the wave vector inside the material is imaginary. In this case the reflection amplitude $\overrightarrow{r_0} = \frac{k-i|k'|}{k+i|k'|}$ is equivalent to a phase, and the square of the amplitude becomes 1 (Total Reflection). Notice here k denotes k_x which is the perpendicular component of the wave vector. The stricter condition for total reflection at *any angle* is $k_x^2 + k_y^2 + k_z^2 < k_c^2$

2.3 Rectangular Barrier

A rectangular barrier is the representation of a layer of material of *perfectly smooth boundaries* and a finite thickness.

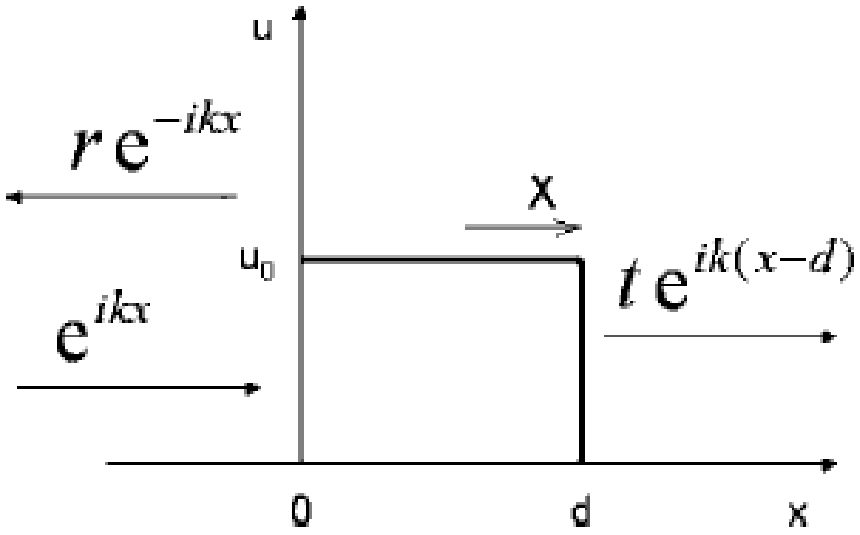

Figure 3: A layer of potential u_0 and thickness d

The Ansatz for the wave function is

$$\psi(x) = \theta(x<0)[e^{ikx} + re^{-ikx}] + \theta(0<x<d)[Ae^{ik'x} + Be^{-ik'x}] + \theta(x>d)[te^{ik(x-d)}] \tag{15}$$

For convenience the transmission amplitude is redefined with an additional phase e^{ikd}. Now it is possible to substitute this Ansatz in the Schrodinger equation and by matching the wave function and its first derivative at points $x = 0$ and $x = d$ we will have 4 equations for the 4 unknown amplitudes r, A, B, t which we can write as a matrix equation and solve. This method however is not one which will use here. The method that will be used as developed in [1] is far more simple and insightful. First we illustrate the details of the notation used in (13) and (14). For any amplitude (reflection or transmission) we have subscript and a directed arrow. The subscript indicates the point at which the amplitude takes action. and the direction indicates the direction of the wave incident on this point. In (13) The notation for the reflection amplitude is for a wave coming from air to the potential u_o at the point 0. From the symmetry of the formula we see that $\overleftarrow{r_0} = -\overrightarrow{r_o}$ where we simply interchange k and k' as now the wave is incident on the interface from inside the layer and a part of it reflects upon the encounter of air ($u = 0$). Using this notation in hand we start to analyze the behaviour of the wave as it travels. The amplitude of the incident wave is

unity. If one could know the amplitude of the wave *inside* the potential that is incident on the interface at d (We denote this amplitude as X). Then the transmission amplitude will simply be

$$t = \overrightarrow{t_d} X \tag{16}$$

That is the amplitude will be reduced by a factor equal to transmission amplitude for a wave that lands on d from the material and gets partially transmitted to air. Similarly the reflection amplitude is composed of two parts
1- The reflection of the incident wave from air at $x = 0$ ($\overrightarrow{r_0}$)
2-The transmission at $x = 0$ of the reflected part of X at $x = d$

$$r = 1\overrightarrow{r_0} + (\overleftarrow{t_0})(e^{ik'd}\overrightarrow{r_d})X \tag{17}$$

The second term is to be understood as follows, X is the amplitude of the wave inside the material travelling towards $x = d$. When the wave arrives at $x = d$ a part of it is reflected back with amplitude $\overrightarrow{r_d}$. As this reflected part travels from $x = d$ to $x = 0$ it picks up a phase $e^{ik'd}$. The wave that arrives at $x = 0$ from inside the material is $(e^{ik'd}\overrightarrow{r_d})X$ and is transmitted with amplitude ($\overleftarrow{t_0}$) hence the contribution to the total reflection amplitude from the second term. The task now is to find X. We know X is the wave amplitude inside the material landing onto $x = d$. There are two ways to do this task both are short in the math but requires thought and consideration of the details of each to appreciate. The first way as in [1] is to write a self-consistent equation

$$X = e^{ik'd}\overrightarrow{t_0} + e^{ik'd}\overleftarrow{r_0}e^{ik'd}\overrightarrow{r_d}X \tag{18}$$

The first term is the transmitted part of the incident wave multiplied by the phase it picks up as it travels from $x = 0$ to $x = d$. The second term is the contribution from X itself as it reflects from $x = d$ and reflects once again from $x = 0$ landing back on $x = d$ multiplied by the corresponding phases for each journey between the two ends. Notice that $\overleftarrow{r_0} = \overrightarrow{r_d}$ and are both equal to $-\overrightarrow{r_0}$ given by (13) which we will simply call r_0 (reflection of a wave coming from air onto the boundary of potential u_0) We can solve (18) for X giving

$$X = \frac{e^{ik'd}\overrightarrow{t_0}}{1 - r_0^2 e^{2ik'd}} \tag{19}$$

Another argument to arrive at (19) is to consider *all the possible journeys* by which the original wave can reach the boundary at $x = d$.
1- The first wave is simply the transmitted part of the incident wave $e^{ik'd}\overrightarrow{t_0}$, let's call this M.
2- The second wave is that where M reflects from $x = d$ travels to $x = 0$, reflects back and travels to $x = d$ given by

$$e^{ik'd}\overleftarrow{r_0}e^{ik'd}\overrightarrow{r_d}M = r_0^2 e^{2ik'd}M \tag{20}$$

3- The same journey for the second wave as for M, and similarly for all consecutive reflections each time multiplying by $r_0^2 e^{2ik'd}$ for the back and forth journey amplitude.
The total wave inside the material arriving at $x = d$ (Which we denoted by X) is therefore given by geometrical series

$$X = M + r_0^2 e^{2ik'd}M + (r_0^2 e^{2ik'd})^2 M + (r_0^2 e^{2ik'd})^3 M + ... = \frac{M}{1 - r_0^2 e^{2ik'd}} = \frac{e^{ik'd}\overrightarrow{t_0}}{1 - r_0^2 e^{2ik'd}} \tag{21}$$

Which is the same formula as in (19). Now that X is known we go back and write the explicit formulas for the total

reflection and transmission amplitudes from the layer.

$$r = r_0 + \frac{\overleftarrow{t_0}\,\overrightarrow{t_0}\,e^{2ik'd}(-r_0)}{1 - r_0^2 e^{2ik'd}} = r_0 \frac{1 - e^{2ik'd}}{1 - r_0^2 e^{2ik'd}} \tag{22}$$

The last form comes from the relation $r_0^2 + \overleftarrow{t_0}\,\overrightarrow{t_0} = 1$ which can be show by direct substitution from the formulas for the amplitudes in terms of the wave vectors k and k'.

$$t = \overrightarrow{t_d} \frac{e^{ik'd}\overrightarrow{t_0}}{1 - r_0^2 e^{2ik'd}} = e^{ik'd} \frac{1 - r_0^2}{1 - r_0^2 e^{2ik'd}} \tag{23}$$

Here we also used $\overrightarrow{t_d}\,\overrightarrow{t_0} = \overleftarrow{t_0}\,\overrightarrow{t_0} = 1 - r_0^2$ as in (22).

2.4 Two Mirrors

The technique we used to find the reflectivity for the potential barrier will now show its robustness when we apply a similar procedure to find the *total reflectivity amplitude* and *total transmission amplitude* for a system of two semi-transparent mirror. We use mirror instead of layer to indicate that the potential is *arbitrary* and we use semi-transparent to indicate that it is *finite*.

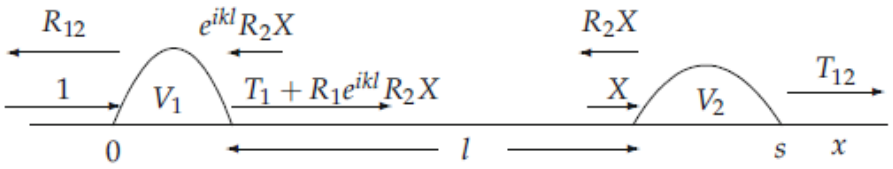

Figure 4: Two semi-transparent mirror separated by a distance l

The goal is to find R_{12} and T_{12} which are the total reflection and the transmission amplitudes from the two mirrors. Here subscripts indicate which mirror since each mirror will be treated as a whole (mirrors replace points in the previous notation). Similarly the amplitude of the incident wave on the first mirror is 1 and the unknown amplitude incident on the second wave is X. By the same arguments we used to write a formula for X in the rectangular potential we write for X

$$X = 1e^{ikl}t_1 + e^{ikl}r_1e^{ikl}r_2X \tag{24}$$

Where here we dropped the arrows as the mirrors are surrounded by air on the left and the right and is assumed to be *symmetrical*. If it were not a right-left symmetrical potential we have to put back the arrows. Solving for X gives

$$X = \frac{t_1e^{ikl}}{1 - r_1r_2e^{2ikl}} \tag{25}$$

The total reflection amplitude is therefore a sum of two parts
1- The reflection of the original incident wave from the first mirror
2- The transmission of the reflected part of X from the second mirror through the first mirror

$$R_{12} = r_1 + t_1e^{ikl}r_2X \tag{26}$$

and the total transmission amplitude is simply the transmission of X through the second mirror

$$T_{12} = t_2 X \tag{27}$$

Explicitly writing the formulas for the amplitudes

$$R_{12} = r_1 + t_1^2 \frac{e^{2ikl} r_2}{1 - r_1 r_2 e^{2ikl}} \tag{28}$$

$$T_{12} = \frac{t_2 e^{ikl} t_1}{1 - r_1 r_2 e^{2ikl}} \tag{29}$$

If the two mirrors were stuck to each other with no separation in between (ie. $l = 0$) the amplitudes become

$$R_{12} = r_1 + t_1^2 \frac{r_2}{1 - r_1 r_2} \tag{30}$$

$$T_{12} = \frac{t_2 t_1}{1 - r_1 r_2} \tag{31}$$

The previous formulas were applied (as will be shown in methodology sections) in the MATLAB program that was used to simulate the reflectivity of neutrons (and X-rays) from multilayered structure Where the previous formulas are applied recursively starting from the substrate and the layer on top of it and recursively considering the total reflectivity and transmission in one cycle as a reflection and transmission from a second "mirror" in the next cycle where the first mirror is the next layer to add to the contribution of reflectivity and transmission.

2.5 A Layer On a Substrate

To apply the formulas in (30) and (31) for the case of one layer on top of an infinitely thick substrate we need to find r_l,t_l, and r_s where l stands for the layer and s stands for the substrate. But we know a layer is a rectangular potential and a substrate is a potential step and we already calculated the reflectivity and transmission of each.

$$r = r_l + t_l^2 \frac{r_s}{1 - r_l r_s} \tag{32}$$

$$t = \frac{t_s t_l}{1 - r_l r_s} \tag{33}$$

Where

$$r_s = \frac{k - k_s}{k + k_s} \tag{34}$$

$$r_l = r_0 \frac{1 - e^{2ik_l d}}{1 - r_0^2 e^{2ik_l d}} \tag{35}$$

$$t_l = e^{ik_l d} \frac{1 - r_0^2}{1 - r_0^2 e^{2ik_l d}} \tag{36}$$

$$r_0 = \frac{k - k_l}{k + k_l} \tag{37}$$

$$k_{l,s} = \sqrt{k^2 - u_{l,s}} \tag{38}$$

Where d is the thickness of the substrate and r_0 is the reflectivity at one boundary of the layer for a wave incident from air. This is the complete system of equations that gives the reflectivity of a layer on top of a substrate in terms of the parameters characterizing the sample (u_l, u_s and d) and the initial incident wave k. As mentioned before after finding this reflectivity we can put on top as many layers as we wish recursively applying (30) to find the collective reflectivity.

2.6 X-ray and Neutrons

Although the Schrodinger equation is not applicable for photons, the analysis that was done on the wave mechanics of neutrons in mirrors and rectangular barriers is still correct for photons as it is in some sense a *kinematical* analysis for the optics and it assumes no special dynamical equation. The formulas for r_0 and t_0 where found for light in terms of refractive indices and incident angles and were known as *Fresnel equations*. The only part that remains is whether the formula $k' = \sqrt{k^2 - u}$ is true for light or no. For neutrons $u = \frac{2mU}{\hbar^2}$. U is the potential of interaction between the neutrons and the nuclei of the atoms in the layers. For photons it represents the potential of interaction between the photons and the *electron cloud* of the atom (Compton effect). One derivation of the form of U is the Fermi pseudo-potential where we assume an interaction between neutrons (photons) and one nucleus (atom) to be a delta function potential localized only at the point where the nucleus (atom) is and is given by $V = b\frac{2\pi\hbar^2}{m}\delta(r)$. The net potential is the average over the whole volume of the layer

$$U = \frac{1}{v}\int_v V\,dr = \frac{2\pi\hbar^2}{m}Nb \tag{39}$$

where N is the number of atoms per unit volume. In this case

$$u = 4\pi Nb \tag{40}$$

$$k'^2 = k^2 - 4\pi Nb \tag{41}$$

This formula can be written in terms of the refractive index $n = \frac{k'}{k}$

$$n^2 = 1 - \frac{\lambda^2}{\pi}Nb \tag{42}$$

The product Nb is termed the *the coherent scattering length density* and it is a measure of the scattering power of the material. For X-ray this quantity is always positive (light slows down) and b is given by $b = Zr_e$ where Z is the atomic number (number of electrons in a neutral atom) and r_e is the classical electron radius given by

$$r_e = \frac{e^2}{4\pi\epsilon_0 m_e c^2} \tag{43}$$

For neutrons it can be either positive or negative. The scattering length density can also have an imaginary component to represent *absorption*. If the the scattering length density has an imaginary part, the wave vector has an imaginary part, and the wave $e^{i\vec{k}\cdot\vec{r}}$ will have a real exponential exponential decay factor which represents the effect of absorption. If the scattering length density of x-ray is used. The formulas derived for the calculation of reflectivity are perfectly valid for X-ray as well (as will be demonstrated in the simulations)

3 Wave Mechanics of Polarized Neutrons

For the previous part neutrons were treated as scalar particles with no intrinsic magnetic moment. Many of the interesting phenomena, experimental techniques and applications arise when we consider the effect of magnetic fields on neutrons. As we didn't invoke much of the spin-relevant effects of the neutrons during the two months of research despite the original final part of the initial plan to use polarized neutrons to examine the coexistence of superconductivity and ferromagnetism in multilayered structures due to anomalies that were encountered in the analysis of the data that later were found to be due to the roughness of the interfaces of the layers (More on that in methodology). The digression on the magnetic effects of neutrons which are plenty enough to produce a whole book about is here cherry-picked in a manner to highlight only parts that are relevant to experimental setup and the simulational framework used. Neutrons are spin $\frac{1}{2}$ particles. That means their total wave function has a *spinor* component, and they interact in a magnetic field with a potential $U_{\pm} = \mp\mu \cdot \mathbf{B}$. where μ is the magnetic dipole moment of the neutron which is proportional to it's spin angular momentum. The magnetic scattering length density $\rho_m = \mp\frac{m}{2\pi\hbar^2}\mu \cdot \mathbf{B}$ therefore the reduced potential that we use in our formula for the wave vector $u_m = 4\pi\rho_m = \mp\frac{2m}{\hbar^2}\mu \cdot \mathbf{B}$ depending on the spin of the neutron. The wave function is now a two component spinor written as

$$|\Psi\rangle = \begin{pmatrix} \psi_u \\ \psi_d \end{pmatrix} = \psi_u |\xi_u\rangle + \psi_d |\xi_d\rangle \tag{44}$$

Where

$$|\xi_u\rangle = \begin{pmatrix} 1 \\ 0 \end{pmatrix} \tag{45}$$

$$|\xi_d\rangle = \begin{pmatrix} 0 \\ 1 \end{pmatrix} \tag{46}$$

are the the spin up/down spinors. They are eigenstates of S_z the spin operator for the z-axis with eigenvalues $\pm\frac{\hbar}{2}$ The magnetic potential is written in terms of the *Pauli matrices*. $U = |\mu_{neutron}|\sigma \cdot \mathbf{B}$ where the plus and minus are now taken care of in the form of the elements of the Pauli matrices.$|\mu_{neutron}| = 1.91\frac{e\hbar}{2mc}$. The Schrodinger equation for a neutron with spin in a magnetic field **B** is

$$i\frac{m}{\hbar}\frac{\partial}{\partial t}|\Psi\rangle = [-\frac{\nabla^2}{2} + \frac{m}{\hbar^2}U - \frac{m}{\hbar^2}\mu \cdot \mathbf{B}]|\Psi\rangle \tag{47}$$

Similar to the previous section we consider only a potential that changes in one direction and is time independent. We also assume the same for the magnetic field (If the magnetic field changes with time we will use the time dependent one dimensional form). A second simplification we do that clarifies the formulas to come is to rescale the time parameter $t' = \frac{\hbar}{m}t$, the magnetic field magnitude $B = \frac{m}{\hbar^2}|\mu_{neutron}|B$, and the potential as before $u = \frac{2m}{\hbar^2}U$. The one dimensional time independent equation becomes (dropping all the primes and using the new rescaled variables as simply t, B and u)

$$(\frac{\partial^2}{\partial x^2} + k^2 - u(x) - 2\sigma \cdot \mathbf{B})|\Psi(x)\rangle = 0 \tag{48}$$

The time independent equation is used to find reflection and transmission through mirrors and multilayered systems with a magnetization. The time dependent equation is used to analyze the behaviour of neutrons in *periodic fields* that are used to change the orientation of the neutron's spin.

3.1 Plane Wave in a Homogeneous Magnetic field

For an incident wave of neutrons in a vacuum that has a magnetic field $\mathbf{B_0}$ the wave function satisfies

$$(-\frac{\partial^2}{\partial x^2} - k^2 + 2\sigma \cdot \mathbf{B_0})\,|\Psi(x)\rangle = 0 \tag{49}$$

If the neutrons have arbitrary polarization

$$|\xi\rangle = \alpha_u\,|\xi_u\rangle + \alpha_d\,|\xi_d\rangle \tag{50}$$

Where $|\alpha_u|^2 + |\alpha_d|^2 = 1$ and the "up" and "down" directions are defined by the direction of the magnetic field. The solution is of the form

$$|\Psi\rangle = \alpha_u e^{ik_u x}\,|\xi_u\rangle + \alpha_d e^{ik_d x}\,|\xi_d\rangle = \begin{pmatrix} \alpha_u e^{ik_u x} \\ \alpha_d e^{ik_d x} \end{pmatrix} \tag{51}$$

Where $k_{u,d} = \sqrt{k^2 \mp 2B_0}$ Now we invoke some of the mathematical properties of the Pauli matrices to write the solution in matrix form. Any function of the form $f(\sigma_z)$ has the same Eigenvectors as the matrix σ_z and its Eigenvalues are $f(\pm 1)$. In this case the previous expression can be simplified to

$$|\Psi(x)\rangle = e^{i\hat{k_0}x}\,|\xi\rangle \tag{52}$$

Where $\hat{k_o} = \sqrt{k^2 - 2\sigma \cdot \mathbf{B_0}}$ is a wave vector matrix and $e^{i\hat{k_0}x}$ is a plane wave matrix.

3.2 Semi-Infinite Magnetic Mirror

For a wave of neutrons initially in a magnetic field $\mathbf{B_0}$ incident on a boundary that has both a magnetic $(\sigma \cdot \mathbf{B_i})$ and nuclear potential u_0 where $\mathbf{B_i}$ is the magnetic field inside the material

$$(-\frac{\partial}{\partial x^2} + u_0\theta(x>0) + 2\sigma \cdot \mathbf{B_0}\Theta(x<0) + 2\sigma \cdot \mathbf{B_i}\Theta(x>0) - k^2)\,|\Psi(x)\rangle = 0 \tag{53}$$

The Ansatz of the solution is

$$|\Psi(x)\rangle = \Theta(x<0)(e^{i\hat{k_0}x} + e^{-i\hat{k_0}x}\hat{r}) + \Theta(x>0)e^{i\hat{k_i}x}\hat{t} \tag{54}$$

where $\hat{r}$ and $\hat{t}$ are reflection and transmission amplitude *matrices.* $\hat{k_i} = \sqrt{k^2 - u - 2\sigma \cdot \mathbf{B_i}}$ By matching the wave function and its first derivative at $x = 0$ we have the following equations

$$\hat{I} + \hat{r} = \hat{t} \tag{55}$$

$$\hat{k_0}(\hat{I} - \hat{r}) = \hat{k_i}\hat{t} \tag{56}$$

solving for $\hat{r}$ and $\hat{t}$

$$\hat{r} = (\hat{k_0} + \hat{k_i})^{-1}(\hat{k_0} - \hat{k_i}) \tag{57}$$

$$\hat{t} = \hat{I} + \hat{r} = (\hat{k_0} + \hat{k_i})^{-1}(2\hat{k_0}) \tag{58}$$

These matrices tell us the probabilities of reflection with and without a flipping of the spin. To illustrate consider initially neutrons polarized along the direction of the initial magnetic field $\mathbf{B_0}$, $|\xi_0\rangle = |\xi_u\rangle$. The diagonal element

$\langle \xi_u | \hat{r} | \xi_u \rangle$ is the probability amplitude for reflection without spin flip and the off-diagonal element is the probability amplitude for reflection with spin flip and similarly for $|\xi_0\rangle = |\xi_d\rangle$. The elements are found by invoking properties of the Pauli matrices and the spinor states.

3.3 Finite Magnetic Mirror

Once the matrix nature of the quantities is understood the previous arguments for the scalar case can be extended taking into consideration the order of multiplication as generally matrices do not commute. Again starting from the formula for $\hat{X}|\xi_0\rangle$ the spinor amplitude of the wave incident on the right end of the barrier and writing $\hat{R}$ and $\hat{T}$ in terms of $\hat{X}$ then substituting the self-consistent formula for $\hat{X}$ we have for the amplitude matrices

$$\hat{R} = \hat{r} - \hat{t}' e^{i\hat{k}_i d} \hat{r} (\hat{I} - e^{i\hat{k}_i d} \hat{r} e^{i\hat{k}_i d} \hat{r})^{-1} e^{i\hat{k}_i d} \hat{t} \tag{59}$$

$$\hat{T} = \hat{t}' (\hat{I} - e^{i\hat{k}_i d} \hat{r} e^{i\hat{k}_i d} \hat{r})^{-1} e^{i\hat{k}_i d} \hat{t} \tag{60}$$

Where

$$\hat{r} = (\hat{k}_0 + \hat{k}_i)^{-1} (\hat{k}_0 - \hat{k}_i) = -\hat{r}' \tag{61}$$

$$\hat{t} = \hat{I} + r \tag{62}$$

$$\hat{t}' = \hat{I} - r \tag{63}$$

Where no prime indicates from air to the layer and the prime indicate from the layer to air (like the arrows in scalar case). Again the elements of the amplitude matrices are obtained in an analytical form using the properties of the Pauli matrices and the spinors or numerically. For elastic scattering the horizontal component of the velocity of the reflected neutrons is conserved. If no spin flip occurs the potential energy of the neutrons in the external magnetic field remains unchanged hence the kinetic energy remains unchanged too so the vertical component of velocity remains the same. If however the spin of the neutrons is flipped the potential energy of the neutrons change and accordingly so does their kinetic energy and vertical component of velocity (as the horizontal is always conserved in elastic scattering). If the neutrons flip from aligned to anti-aligned after reflection they lose potential energy hence their vertical component of velocity increases. If neutrons flip from anti-aligned to aligned after reflection they gain potential energy and therefore their vertical component of velocity decreases. This results in a small *triple splitting* of the reflected beam given by the formula $\Delta\theta = \frac{k_\perp}{k} \approx \pm \frac{B}{E\theta}$ where E is the energy of the neutrons, θ is the incidence angle, and $\Delta k_\perp = \sqrt{k_\perp^2 \pm 4B} - k_\perp$

3.4 Two Magnetic Mirrors

The results for two magnetic mirrors is identical to that of non-magnetic ones and obtained by the same argument on the amplitude $\hat{X}$ of the wave incident on the second mirror except for the obvious difference of matrix notation. If the two mirrors are right next to each other ($l = 0$) and mirror i has reflection and transmission amplitudes $\hat{r}_i$ and $\hat{t}_i$ the total reflection and transmission amplitudes are given by

$$\hat{R_{12}} = \hat{r}_1 + \hat{t}_1 \hat{r}_2 (\hat{I} - \hat{r}_1 \hat{r}_2)^{-1} \hat{t}_1 \tag{64}$$

$$T_{12} = \hat{t}_2 (\hat{I} - \hat{r}_1 \hat{r}_2)^{-1} \hat{t}_1 \tag{65}$$

3.5 Polarizing Neutrons

There are 3 experimental methods for the polarization of neutrons
1- Reflection from magnetized mirrors
2- Transmission through magnetized mirrors
3- Transmission through polarized gas
In the first two methods neutrons interact via the optical potential which is the sum of nuclear potential and magnetic potential. The potential is higher for neutrons that are along the magnetic field ($u+2B$) and lower for neutrons that are aligned against the magnetic field ($u-2B$). Assuming the external and internal magnetic fields are collinear the medium reflects all neutrons polarized along the magnetic field and transmits the ones polarized against the magnetic field except when the momentum of the incident wave perpendicular to the interface is within the range$\sqrt{u-2B} \leq k_{\perp} \leq \sqrt{u+2B}$ in this case some neutrons polarized against the field are reflected. In some experimental setups the neutrons are reflected *multiple times* where the number reflected neutrons that are polarized against the magnetic field decays to zero. The mirrors give a high degree of polarization but low output intensity for thermal neutrons due the very small angle of incidence. For polarized gases the beam is transmitted through the polarized nuclei where the nuclei absorbs oppositely polarized neutrons and does not absorb neutrons of the same polarization. This absorption is accompanied by a strong loss in the transmitted beam however it can be used for beams of large spatial spread and wavelength range and the lower the neutrons' energy the higher the polarizing effect of the gas. A polarized gas like helium which can be polarized through pumping of Rubidium vapor which transfers its polarization to helium through collision can remain polarized for several days at room temperature. If the beam is within a narrow wavelength range and is well-collimated magnetic crystals can be used for polarization. Another experimental devices that are used during experiments with polarized neutron are *analyzers*. Analyzers work with the same basic principles of polarizers and are used as polarization filters. For the case of mirrors they reflect neutrons polarized along the field and transmit those polarized against the field. For transmission through polarized gases as He the analyzer transmits neutrons polarized along the direction of polarization of the nuclei.

3.6 Spin Flippers

One of the most important experimental devices used for manipulation of polarized neutron are spin flippers. If the neutrons are in a slowly space varying magnetic field (Adiabatic change) the angle α between the magnetic field **B** and the spin vector of the neutron s is conserved (that is to say the spin orientation chases the changing magnetic field keeping an equal separation angle). The angular velocity of the magnetic field is given by

$$\Omega = \frac{1}{B}\vec{v}\cdot\frac{d\mathbf{B}}{dr} \tag{66}$$

where $\vec{v}$ is the velocity of the neutron. The neutron itself executes a *Larmor precession* around the direction of the magnetic field with a frequency

$$\omega = \frac{\mu}{\hbar}B \tag{67}$$

The ration $\frac{\Omega}{\omega}$ is called *the adiabatic parameter*. The smaller the adiabatic parameter the stricter the conservation of the angle α. If however the change of the magnetic field is abrupt and sudden the spin arrow s can't keep up with **B** and suddenly flips direction with respect to the magnetic field. This is the basic principle of operation for spin flippers. This non-adiabatic process can be done in two ways
1- A time-independent magnetic field rapidly oscillating in space (A direct current magnetic field that abruptly

flips the direction of the magnetic field in space)
2- A combination of constant and oscillating magnetic fields (Radio Frequency magnetic fields)
For the first technique there are 3 famous methods
i) Neutrons pass through a thin metallic film with electric current passing parallel to the film's surface. The magnetic field from the current is opposite on the opposite faces of the film. The neutrons retain the direction of the flipped field after passing through the film. This is known as the *current foil method*
ii) The flipper consists of two current carrying coils placed opposite to each other. The magnetic field vanishes in the region between the coils as the two magnetic fields from the two coils cancel each other. As the neutrons enter this region their spin is unchanged while the direction of the magnetic field is changed. This method is called the *zero field method*
iii) The third kind of DC rotators were first invented by *Mezei* using time-independent fields. This flipper can be used to rotate the spin around any axis. The magnetic field is produced by two oppositely oriented coils placed side by side *perpendicular* to the neutron beam. The magnitude of the magnetic field inside the coils is sat the same as the magnitude of the external magnetic field which is orthogonal to both the beam and the opposite magnetic fields of the coils. Assume initially the external magnetic field and the polarization of the neutrons is along the z-axis and the direction of the magnetic fields of the two coils are along -x and +x axis, if the neutron spins precess an angle 2ϕ around the total magnetic field after crossing the first coil the new spin state of the neutrons become

$$|\xi_1\rangle = e^{\frac{i[\sigma_z-\sigma_x]\phi}{\sqrt{2}}}|\xi_u\rangle \tag{68}$$

and after crossing the second coil

$$|\xi_2\rangle = e^{\frac{i[\sigma_z+\sigma_x]\phi}{\sqrt{2}}}|\xi_1\rangle = e^{\frac{i[\sigma_z+\sigma_x]\phi}{\sqrt{2}}}e^{\frac{i[\sigma_z-\sigma_x]\phi}{\sqrt{2}}}|\xi_u\rangle = (cos^2(\phi)\hat{I}+\sqrt{2}icos(\phi)sin(\phi)\sigma_Z - isin^2(\phi)\sigma_y)|\xi_u\rangle \tag{69}$$

If $\phi = \frac{\pi}{2}$ then $|\xi_2\rangle = -|\xi_u\rangle$ and the spin is flipped upside down. The rapid change in the magnetic field occurs as the neutrons pass through the coil walls. By changing the size of coils, their orientation and the relative magnitudes of the internal and external fields the neutrons' spin can be flipped to any orientation. This method is only functional when the neutrons are within a narrow velocity range as they depend on the flight time of the neutrons through the coils. Three examples of Spin Flippers are shown below

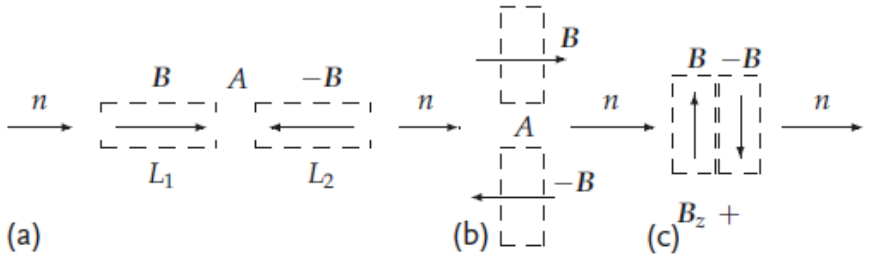

Figure 5: (a) and (b) are examples of "zero field" spin flippers. (c) is a Meizei spin flipper

The Radio Frequency (RF) flippers are more interesting and worth examining in detail compared to DC flippers. The unique property of RF fields is the change in the neutron's energy through absorption or emission of RF radiation quanta. In the presence of a RF field the neutrons obey the *time-dependent* Schrodinger equation

$$i\frac{\partial}{\partial t}|\Psi(t,x)\rangle = [-\frac{1}{2}\frac{\partial^2}{\partial x^2}+\frac{u(x)}{2}+\sigma\cdot\mathbf{B_0}(x)+\sigma\cdot\mathbf{B_{rf}}(t,x)]\,|\Psi(t,x)\rangle \tag{70}$$

For the ideal conditions when the field is extended only over a finite region of space (*Kruger* configuration)

$$\mathbf{B_0}(x) + \mathbf{B_{rf}}(t,x) = \Theta(0 \leq x \leq D)[\mathbf{B_0} + \mathbf{B_{rf}}(t)] \tag{71}$$

For simplicity we assume $u = 0$. The magnetic field components are given by

$$\mathbf{B_0} = (0, 0, B_0) \tag{72}$$

$$\mathbf{B_{rf}} = (cos(2\omega t), sin(2\omega t), 0) \tag{73}$$

A schematic diagram of the setup is shown below with the behaviour of the wave upon encountering the magnetic potential

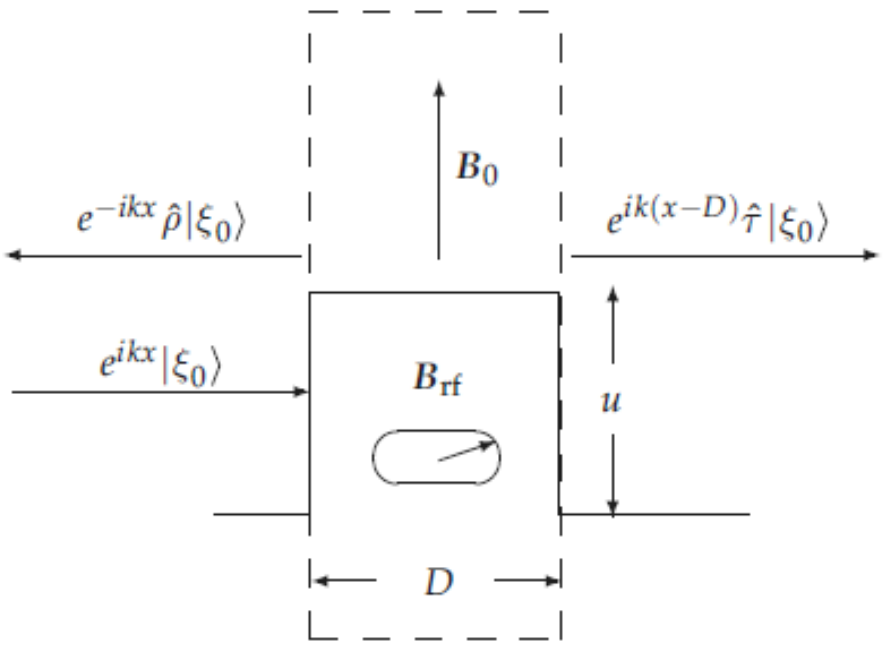

Figure 6: RF spin flipper

The incident wave is given by $\Theta(x < 0)e^{ik_0 x - iE_0 t}|\xi_0\rangle$ where $E_0 = \frac{k_0^2}{2}$. In the common case when $E_0 >> B_0 >> B_{rf}$ (the velocity of the neutrons is not changed significantly as it enter the magnetic region) a formula can be obtained for the probability of the flipping of the neutron spin w_{fl} assuming it is initially aligned with the magnetic field $\mathbf{B_0}$.

$$w_{fl} = \frac{B_{rf}}{B_{rf}^2 + (\omega - B_0)^2} sin^2(\sqrt{B_{rf}^2 + (\omega - B_0)^2}\, t_1) \tag{74}$$

Where $t_1 = \frac{D}{K_0}$. When $\omega = B_0$ and $t_1 B_{rf} = n\pi + \frac{pi}{2}$ the probability of spin flip is 1 (hence the other name "resonant" spin flipper for the technique).
From (74) if $\omega = B_0$

$$w_{fl} = sin^2(B_{rf} t_1) \tag{75}$$

The probability of spin flip is dependent on the *time of flight* of the neutrons through the coil $t_1 = \frac{l}{v_0}$ where v_0 is the

velocity of the neutrons and l is the thickness of the coil. For unpolarized neutrons of kinetic energy comparable to the magnetic energy the velocity of the neutrons for polarization aligned with the field and against the field are not the same. $v_+ = \sqrt{v_0^2 - 2B_0}$ and $v_- = \sqrt{v_0^2 + 2B_0}$. The neutrons aligned with the magnetic field *slow down* and those aligned against it *accelerate* therefore the time of flight for the oppositely aligned neutrons is different (what happens when this separation becomes very large?). This difference can be exploited to completely polarize a neutron beam. If the coil thickness is chosen such that $B_{rf}t_+ = \pi$ and $B_{rf}t_- = \frac{\pi}{2}$ all neutrons aligned with the magnetic field remain unchanged and those aligned against it are flipped so that the transmitted neutrons are all aligned with the magnetic field. Similarly this process can be carried out with a coil thickness that gives $B_{rf}t_+ = \frac{3\pi}{2}$ and $B_{rf}t_- = \pi$ is chosen so that the transmitted neutrons are all aligned against the magnetic field.

3.7 The Echo of Spin

A neutron spin echo experiment is a fantastic illustration and application of all that was discussed previously (and more that wasn't). The magnetic optical analysis, the time-of-flight analysis and velocity selection, polarizers and analyzers, and finally RF spin flippers all come into action in a spin echo experiment. The spin echo technique was first invented by *Meizei* who also invented the Meizei flipper (fig. 5-c). A demonstration of a spin echo experiment [4] is shown below

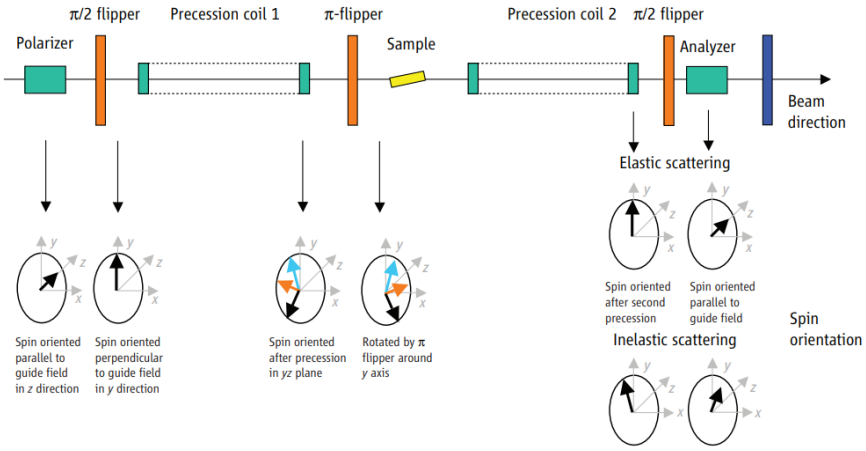

Figure 7: A typical spin echo experiment

Incident neutrons are within a small spectral range (this is achieved using velocity selectors as those discussed in 1.4). The neutrons are polarized to initially have spin in the z-direction. The neutrons are then passed through an RF flipper where all the neutrons' spin are flipped by 90°to align along the y-axis. The neutrons then enter a *precession region* where they will execute Larmor preccesion. Neutrons of different velocities will have acquired *phases* depending on their velocity. This is a process of *dephasing* the neutrons. After the neutrons spin arrow have rotated by the phase corresponding to its velocity the neutrons' spin is flipped by 180° . Now as the neutrons enter a second precession region each neutron will be rotating counter to its first precession direction *reversing* the phase it obtained. If the lengths of the precession regions are chosen such that the phase acquired in the first precession region is exactly compensated by the phase acquired (in the opposite direction) in the second region *all* spins will finish aligned along the y-axis where using a third flipper which rotates the spin by 90° will result in the neutrons arriving all aligned back to their original spin orientation. This is the echo of the spin. Notice this process is independent of the neutrons' velocity as each neutron's spin arrow will have to travel back the phase it acquired

each with the same velocity it acquired it with and in the opposite direction. A good analogy is a rabbit and a turtle that are made to race and as they are both running (off course the rabbit travelled a further distance) a bullet is shot in the air and the start line is now the finish line. Neglecting the time it takes the turtle to turn around, each of them will have to run back the same distance it ran during *a certain time* so they will both reach the point where they started at the same time. Now how does the sample affect this process? The answer is that the complete recovery of the initial polarization (the echo) only happens for neutrons that are elastically scattered from the sample where their velocity remains unchanged. For neutrons that scatter inelastically the final polarization is *tilted* from the initial one and the magnitude of the tilt encodes information regarding the internal dynamics of the sample.

4 Method

This section is an illustration of the simulational work that was done during the two month period of collaboration. The ultimate goal was the analysis of ferromagnetic samples that contained superconducting layers to understand the effect of superconductivity on ferromagnetism. This final purpose was hindered due to the unsatisfactory fit between experimental and theoretical curves which redirected the purpose of the work to improving the simulational program to account for the roughness of the surfaces of the layers which was done to a good degree of success greatly improving the fit of the simulations for X-rays to match that of an already available X-ray fitting program (X'pert reflectivity).

4.1 Plan A

The original plan for the line of work was the following
1- Fit the simulated X-ray reflectivity of the different samples with the corresponding nominal structure and the experimental data using *X'pert reflectivity* simulation and fitting program obtaining information about the values of the real parameters of the structure (densities, thicknesses, etc.).
2- Use the found real parameter (which should typically be close to those of the nominal structures) to model reflectivity of neutrons from the samples and compare them to the experimental data of the neutrons.
3- Study the collective Magnetic/Superconducting behavior of the elements in the samples using the magnetic properties of the neutron beam.
The first step was carried out for 3 samples out of 4 obtaining a good fit for 2 of them and a decent fit for the third.

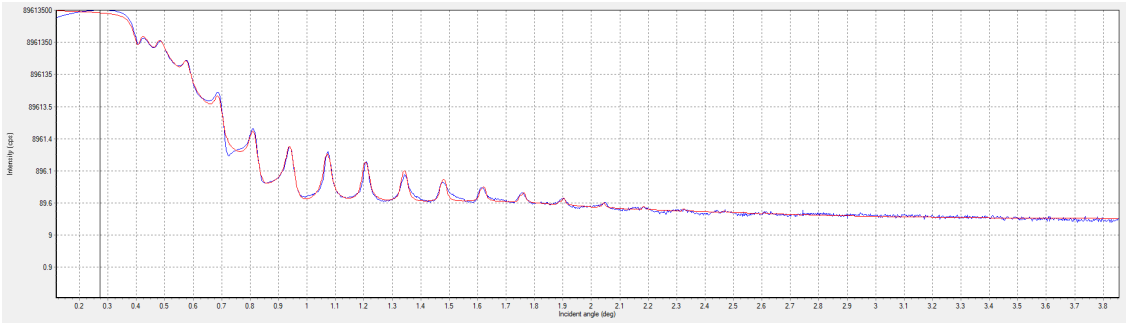

Figure 8: Example of the fitting of samples using X'pert reflectivity. Sample's nominal structure is Al2O3(Substrate)/[Nb(250 A)/Dy(60 A)]x12/Nb(50 A)

The drop of experimental reflectivity at very small angles is due to the *footprint effect* where the footprint of the beam (the horizontal distance on the sample's plane between where the lower end of the beam reaches the plane

and where the higher end of the beam reaches the plane given by $footprint = \frac{d}{sin\theta}$ where d is the thickness of the beam and θ is the incidence angle) is larger than the size of the sample so some neutrons don't fall on the sample. Afterwards, values for the real parameters of the sample were used to model the reflection of neutrons. Counter to expectations the neutrons' modeling were not in good fit with the experimental data of the reflection of neutrons from the same samples (apparent correspondence in Bragg peaks but a mismatch in the values of the critical wavelength which is of critical importance in the determination of the goodness of the fit). We were led to the conclusion to first attempt to model the reflection of X-ray with the same MATLAB program (developed by Dr. Zhaketov) that we used to model the reflection of neutrons. The task was rather straightforward as it was a question of simply using the scattering length density of X-rays instead of neutrons' (as discussed in 2.6) since the program calculates reflectivity in a specular manner similar to optical reflection using an approach to the wave analysis developed in [1]. Such an approach is dependent only on the thickness and potential of each layer assuming perfectly smooth potential boundaries between layers. After implementing the scattering length densities of X-ray for each layer and simulating the reflectivity with the same parameters as fitted by X'pert Reflectivity the simulations did not match between the two programs. As we soon found out that not only did the simulations of X'pert Reflectivity were changing significantly for tweaks in densities and thicknesses, They were also sensitive to changes in the roughness of the layers which the program concurrently fits.

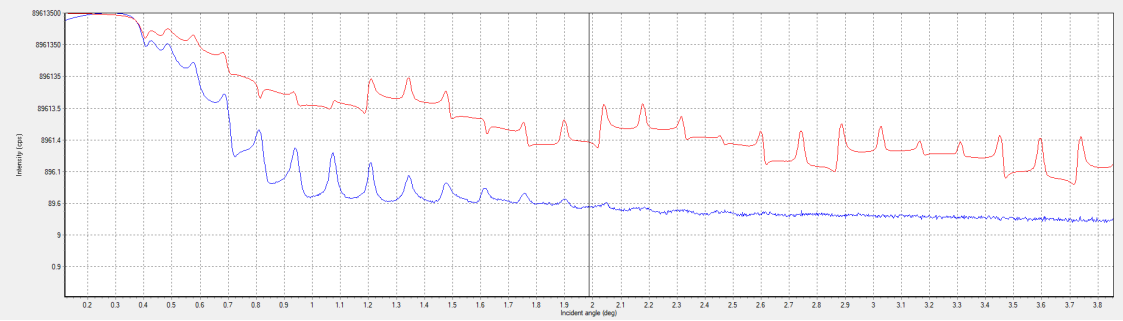

Figure 9: Same fitted sample as figure 8 setting roughness=0 for all layers showing the sensitivity of the fit to roughness

In fact when setting roughness of all layers=0 the goodness of fit decreased drastically, but the simulations were in a very good match with those of the MATLAB program.

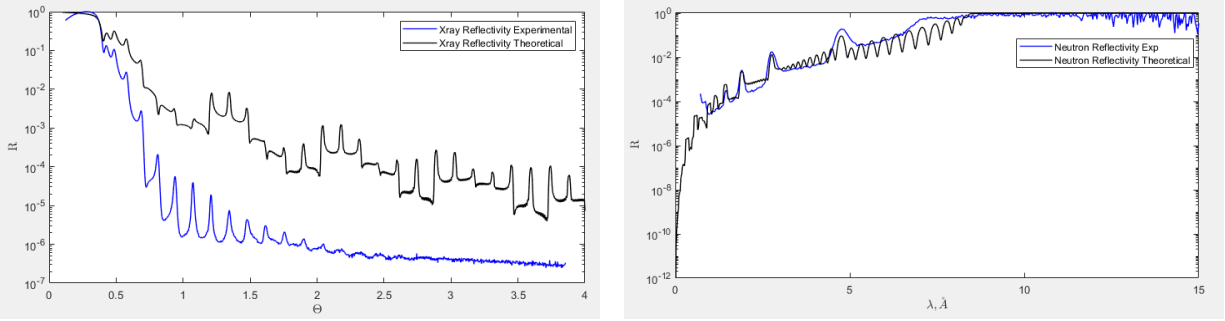

(a) X-ray simulation

(b) Neutrons' simulation

Figure 10: Sample simulated on MATLAB for Neutrons and X-ray reflectivity using the same parameters as fitted from X'pert Reflectivity before including the effect of roughness plotted with the corresponding experimental results

The agreement between the simulations of both programs when roughness is sat to 0 in X'pert Reflectivity is shown below

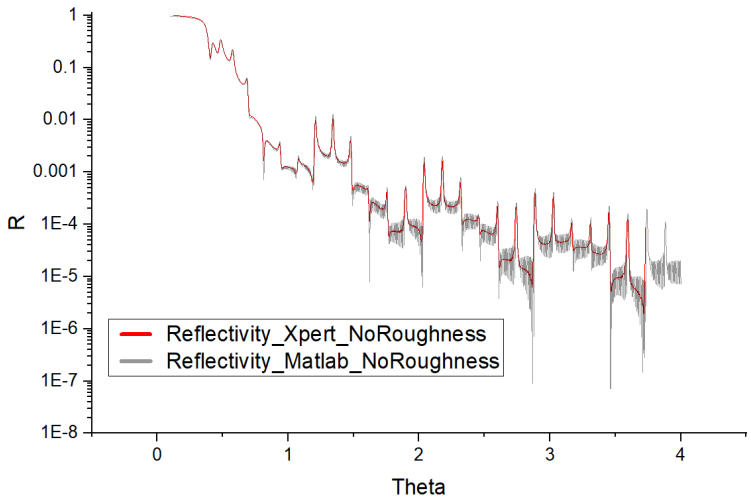

Figure 11: Simulation of the sample from both X'pert Reflectivity and Matlab (No Roughness)

The smaller oscillations on the grey curve can be reproduced in the red curve using a larger number of divisions for the angle in the MATLAB simulation at the cost of longer runtime or can be smoothed out to lie flat along the red curve using a smoothing function. It became apparent that the MATLAB program can be used for X-rays and produce similar results to those in X'pert Reflectivity. However an account of roughness of the surfaces was a *MUST DO*.

4.2 Plan B

Hence the plan was modified to be as follows
1- Add the effect of roughness to the calculation of X-ray and neutron reflectivity to the MATLAB program so that both simulations can be done on the same program.
2- Simultaneously perform fitting for the parameters of the layers of the samples so as to produce values which give a good fit for both X-ray and neutron reflectivity data adding the sum of both the root mean squared errors of the modeled X-ray and neutron reflectivity as compared to their corresponding experimental results.
3- Study the collective Magnetic/Superconducting behavior of the elements in the samples using the magnetic properties of the neutron beams.

4.3 Roughness of Interfaces

The first approach to step 1 was subdividing each layer into many sublayers and assuming a Gaussian distribution of the potential of each main layer thereby having different values of the potentials of the sublayers at parts near the boundaries of each main layer (modulated by a Gaussian form) and converging to the value of the original constant potential of the main layer as the sublayers considered become closer to the middle of the main layer thereby smoothing the transition of the potential between the main layers. The following formula was used to

smooth the transition between the midpoint of layer j and the midpoint of the next layer j+1

$$u(z) = \frac{1}{2}[u_j(1 + erf(\alpha \frac{z_{j+1} - z}{\sigma_{j+1}})) + u_{j+1}(1 - erf(\alpha \frac{z_{j+1} - z}{\sigma_{j+1}}))] \tag{76}$$

z_{j+1} is the position of layer j+1, u_j and u_{j+1} are the potentials of the corresponding layers, σ_{j+1} is the roughness of the j+1 layer which is the interface between the two layers, α is a scale parameter for the error function to control the transition gradient between the two layers. The formula applied in a loop over layers $\forall$ points z between the midpoints of the two layers taking $z = 0$ as the *midpoint* of layer j.

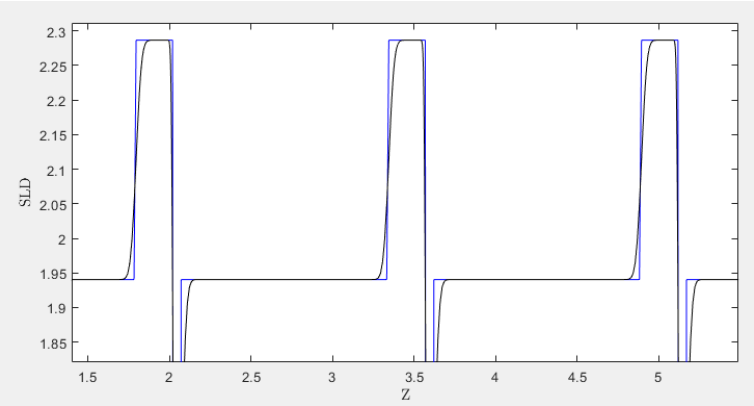

Figure 12: Using error function to smooth the transition between potential boundaries by subdividing each layer into 100 sublayers. $\alpha = 2\sqrt{2}$(The potential is shown for a part of the superlattice for finer details)

After attempting such an approach the fitting showed little improvement. The method was highly time consuming to run simulations compared to the original run-time which made it clear that applying this method for step 2 (fitting) would be an inefficient and computationally tedious process as during fitting simulations are usually redone with slightly modified parameters thousands of times to approach values which result in a good fit.

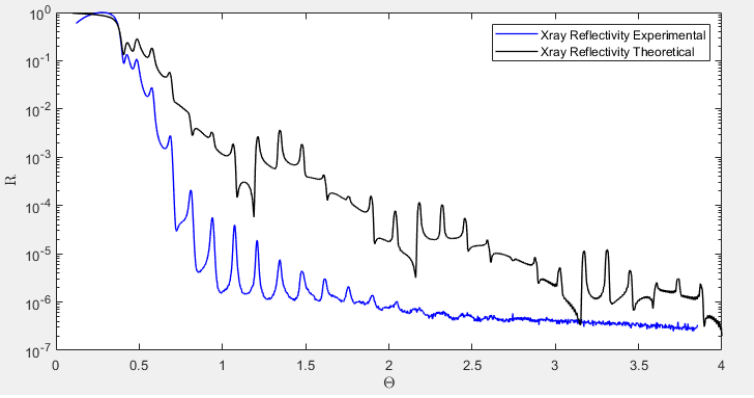

Figure 13: The effect of using error function transition between boundaries on the reflectivity simulation

The second approach was to include a Nevot-Croce factor [2] which is similar to a phenomenological Debye-Waller factor (temperature factor which accounts for the non-ideal positioning of atoms due to vibrations). The factor is an exponentially decreasing coefficient that reduces the reflection amplitude of each layer based on the square of its roughness(σ^2). For a semi-infinite potential barrier of incident wave vector k and a wave vector inside the layer

k' and roughness σ at the interface the reflection amplitude is changed according to the following relation

$$r_{rough} = r_{smooth} e^{-2kk'\sigma^2} \tag{77}$$

The application of the Nevot-Croce factor to simulations of reflectivity by commonly used approaches such as the Parratt formalism are straightforward. However the inclusion of the factor in the Ignatovich calculation which the MATLAB program uses was not as straightforward. After several attempts we succeeded in adding the coefficient (It was found that we needed two different Nevot-Croce factors for two different reflection amplitude components in the reflection amplitude formula of each layer. One from its left -Assuming left to right structure- which depends on the roughness of the layer and one from its right which depends on the roughness of the next layer). The fitting improved drastically becoming more similar to that of X'pert reflectivity except for small effects which X'pert reflectivity takes into account during fitting such as the divergence of the beam and the background intensity of X-ray and neutrons.

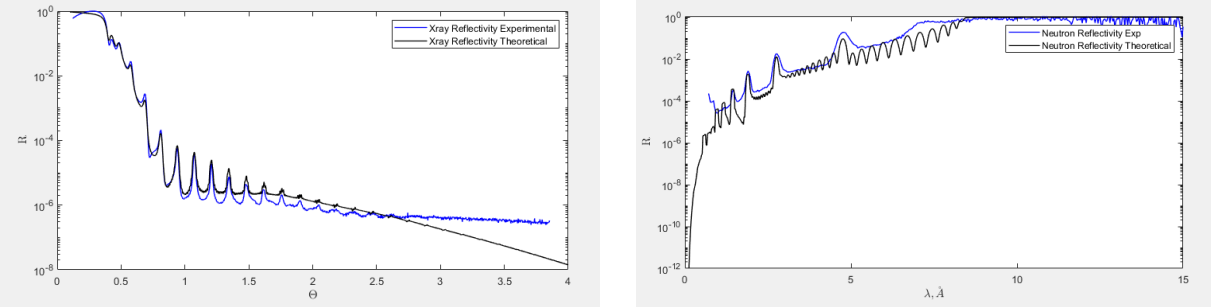

(a) X-ray simulation

(b) Neutrons' simulation

Figure 14: Reflectivity simulation after using the Nevot-Croce factor to account for roughness

Despite the success of the method for the improvement of the fit for X-ray a downside of the Nevot-Croce factor is that it is only applicable when the square roughness is small compared to the reduced critical wavelength (small roughness). After further investigation we found a third solution to the problem of including the effect of roughness on the reflectivity. This solution was developed by Ignatovich [3] and it is similar to the first approach of smoothing the transition between the layers' boundaries except that the approach is not numerical by simply dividing the layer into many sub-layers but rather an analytical one where two *Eckart* functions of the form $U(x) = \frac{U_0}{1+e^{-\frac{x}{h}}}$ with new parameters to be included in the fitting which are related to the roughness of the layers are used to smooth the transition of the potential between the boundaries and as in [3] a complete analytical solution of the reflectivity of a layer on a substrate was obtained substituting the mentioned potentials in the Schrodinger equation. This approach was shown to be 7 times faster than numerical methods and of higher precision and with none of the previously mentioned deficiencies of the other approaches. The only downside of this approach which is incidentally a consequence of its analyticity and robustness is that it is considerably more difficult to implement in a simulation (for example the requirement of the calculation of hypergeometric functions) and would require time and a complete reconstruction of the majority of the functions responsible for the calculation of reflectivity.

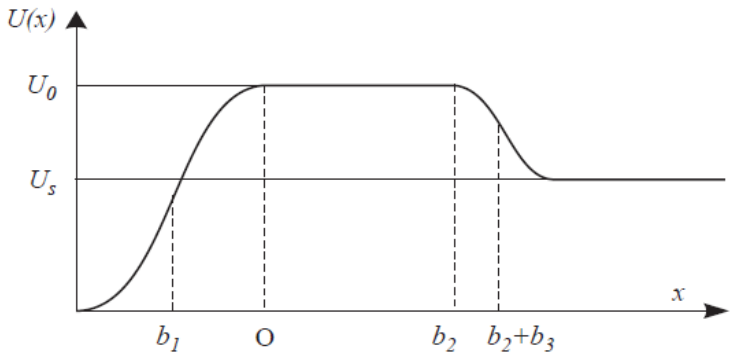

Figure 15: A layer on a substrate with the potential transition between boundaries smoothed using two Eckart functions

5 Conclusion

Although the work with the experimental data was not carried to completion due to the inconvenience of the fit between simulations for neutrons and their corresponding experimental result, the simulations and examination of the effects of different parameters on the reflectivity curve have shown the importance of the roughness factor. The Nevot-Croce correction despite its limitations gave insight into how the fit of the simulated data can be significantly improved when taking roughness into account. It also became apparent that measurements and calculations of non-specular reflection (diffuse scattering) is crucial to the examining of the details of the surface roughness and even for the estimation of the specular scattering itself where in some cases the non-specular component is larger than the specular one [5].

6 Acknowledgements

I'm humbly thankful to Joint Institute for this wonderful research experience, Dr. Vladimir Zhaketov for priceless lessons, knowledge and insights throughout the period of collaboration, and to my University professor Dr. Hisham Anwar for guidance in my first research thesis on Neutron stars which sparked my interest in the study of Neutrons and his constant invaluable support.

7 References

[1] Utsuro, M., & Ignatovich, V. K. (2010). Handbook of neutron optics. John Wiley & Sons.

[2] Nevot, 1., & Croce, P. (1980). Caractérisation des surfaces par réflexion rasante de rayons X. Application à l'étude du polissage de quelques verres silicates. Revue de Physique appliquée, 15(3), 761-779.

[3] Korneev, D. A., Ignatovich, V. K., Yaradaykin, S. P., & Bodnarchuk, V. I. (2005). Specular reflection of neutrons from potentials with smooth boundaries. Physica B: Condensed Matter, 364(1-4), 99-110.

[4] Mesot, J. (2006). The neutron spin-echo technique at full strength. Science, 312(5782), 1888-1889.

[5] Sinha, S. K., Sirota, E. B., Garoff, A. S., & Stanley, H. B. (1988). X-ray and neutron scattering from rough surfaces. Physical Review B, 38(4), 2297.